Computational Science and Its Application, ICSSA 2019 proceedings, Part I, LNCS 11619, pp.322-226, ISSN 0302-9743, ISBN 978-3-030-24288-6, Springer, 2019, https://doi.org/10.1007/978-3-030-24289-3_24

A new Strategy for Scattered Data Approximation Using Radial Basis Functions Respecting Points of Inflection

Martin Cervenka *, Michal Smolik, and Vaclav Skala

Faculty of Applied Sciences, University of West Bohemia,
Plzen, Czech Republic
{cervemar,smolik,skala}@kiv.zcu.cz

Abstract. The approximation of scattered data is known technique in computer science. We propose a new strategy for the placement of radial basis functions respecting points of inflection. The placement of radial basis functions has a great impact on the approximation quality. Due to this fact we propose a new strategy for the placement of radial basis functions with respect to the properties of approximated function, including the extreme and the inflection points. Our experimental results proved high quality of the proposed approach and high quality of the final approximation.

Keywords: Radial basis functions; approximation; stationary points.

1 Introduction

The Radial basis functions (RBF) are well known technique for scattered data approximation in d-dimensional space in general. a significant adventage of the RBF application is its computational complexity, which is nearly independent of the problem dimensionality. The formulation is leading to a solution of a linear system of equations $\boldsymbol{Ax} = \boldsymbol{b}$. There exists several modifications and specifications of the RBF use for approximation. The method of RBF was originally introduced by Hardy in a highly influential paper in 1971 [8], [9]. The paper [8] presented an analytical method for representation of scattered data surfaces. The method computes the sum of quadric surfaces. The paper also stated the importance of the location of radial basis functions. This issue is solved by several papers. Some solutions are proposed by the papers [16], [15], [3], which use the regularization in the forward selection of radial basis function centers. The paper [31] presents an improvement for the problem with the behavior of RBF interpolants near boundaries. The paper [13] compares RBF approximations with different radial basis functions and different placement of those radial basis functions. However, all the radial basis functions are placed with some random or uniform distribution. A bit more sophisticated placement is presented in [14].

* The research was supported by projects Czech Science Foundation (GACR) No. 17-05534S and partially by SGS 2019-016.

Computational Science and Its Application, ICSSA 2019 proceedings, Part I, LNCS 11619, pp.322-226, ISSN 0302-9743, ISBN 978-3-030-24288-6, Springer, 2019, https://doi.org/10.1007/978-3-030-24289-3_24

The selection of a shape parameter is another problem. Wrong selection of this parameter can lead to an ill-conditioned problem or to an inaccurate approximation. The selection of the best shape parameter is thus very important. Fornberg and Wright [5] presents an algorithm which avoids this difficulty, and which allows numerically stable computations of Multi-Quadric RBF interpolants for all shape parameter values. The paper [29] derives a range of suitable shape parameters using the analysis of the condition number of the system matrix, error of energy and irregularity of node distribution. A lot of approaches for selection of a good value of the shape parameter use some kind of random generator. Examples of this approaches are [20], [2]. The paper [1] proposes a genetic algorithm to determine a good variable shape parameter, however the algorithm is very slow.

2 Radial Basis Functions

The Radial basis function (RBF) is a technique for scattered data interpolation [17] and approximation [4], [27]. The RBF interpolation and approximation is computationally more expensive compared to interpolation and approximation methods that use an information about mesh connectivity, because input data are not ordered and there is no known relation between them, i.e. tessellation is not made. Although RBF has a higher computational cost, it can be used for d-dimensional problem solution in many applications, e.g. solution of partial differential equations [11], [33], image reconstruction [28], neural networks [10], [7], [32], vector fields [24], [26], GIS systems [12], [18], optics [19] etc. It should be noted that it does not require any triangulation or tessellation mesh in general. There is no need to know any connectivity of interpolation points, all points are tied up only with distances of each other. Using all these distances we can form the interpolation or approximation matrix, which will be shown later.

The RBF is a function whose value depends only on the distance from its center point. Due to the use of distance functions, the RBFs can be easily implemented to reconstruct the surface using scattered data in 2D, 3D or higher dimensional spaces. It should be noted that the RBF interpolation and approximation is not separable by dimension. For the readers reference a compressed description of the RBF is given in the following paragraphs, for details consider [25], [26].

Radial function interpolants have a helpful property of being invariant under all Euclidean transformations, i.e. translations, rotations and reflections. It does not matter whether we first compute the RBF interpolation function and then apply a Euclidean transformation, or if we first transform all the data and then compute the radial function interpolants. This is a result of the fact that Euclidean transformations are characterized by orthonormal transformation matrices and are therefore two-norm invariant. Radial basis functions can be divided into two groups according to their influence. The first group are "global" RBFs [21]. Application of global RBFs usually leads to ill-conditioned system, especially in the case of large data sets with a large span [13], [23]. An example of

Computational Science and Its Application, ICSSA 2019 proceedings, Part I, LNCS 11619, pp.322-226, ISSN 0302-9743, ISBN 978-3-030-24288-6, Springer, 2019, https://doi.org/10.1007/978-3-030-24289-3_24

"global" RBF is the Gauss radial basis function.

$$\varphi(r) = e^{-\epsilon r^2}, \tag{1}$$

where r is the distance of two points and ϵ is a shape parameter.

The "local" RBFs were introduced in [30] as compactly supported RBF (CSRBF) and satisfy the following condition:

$$\begin{aligned} \varphi(r) &= (1-r)_+^q P(r) \\ &= \begin{cases} (1-r)^q P(r) & 0 \le r \le 1 \\ 0 & r > 1 \end{cases} \end{aligned} \tag{2}$$

where $P(r)$ is a polynomial function, r is the distance of two points and q is a parameter.

2.1 Radial Basis Function Approximation

RBF interpolation was originally introduced by [8] and is based on computing the distance of two points in any k-dimensional space. The interpolated value, and approximated value as well, is determined as (see [22]):

$$h(\boldsymbol{x}) = \sum_{j=1}^{M} \lambda_j \varphi(\|\boldsymbol{x} - \boldsymbol{\xi}_j\|) \tag{3}$$

where λ_j are weights of the RBFs, M is the number of the radial basis functions, φ is the radial basis function and $\boldsymbol{\xi}_j$ are centers of radial basis functions. For a given dataset of points with associated values, i.e. in the case of scalar values $\{\boldsymbol{x}_i, h_i\}_1^N$, where $N \gg M$, the following overdetermined linear system of equations is obtained:

$$h_i = h(\boldsymbol{x}_i) = \sum_{j=1}^{M} \lambda_j \varphi(\|\boldsymbol{x}_i - \boldsymbol{\xi}_j\|) \quad \text{for } \forall i \in \{1, \dots, N\} \tag{4}$$

where λ_j are weights to be computed; see Fig. 1 for a visual interpretation of (3) or (4) for a $2\frac{1}{2}D$ function. Point in $2\frac{1}{2}D$ is a $2D$ point associated with a scalar value.

Equation (4) can be rewritten in a matrix form as

$$\boldsymbol{A}\boldsymbol{\lambda} = \boldsymbol{h}, \tag{5}$$

where $A_{ij} = \varphi(\|\boldsymbol{x}_i - \boldsymbol{\xi}_j\|)$ is the entry of the matrix in the $i-$th row and $j-$th column, the number of rows $N \gg M$, M is the number of unknown weights $\boldsymbol{\lambda} = [\lambda_1, \dots, \lambda_M]^T$, i.e. a number of reference points, and $\boldsymbol{h} = [h_1, \dots, h_N]^T$ is a vector of values in the given points. The presented system is overdetermined, i.e. the

Computational Science and Its Application, ICSSA 2019 proceedings, Part I, LNCS 11619, pp.322-226, ISSN 0302-9743, ISBN 978-3-030-24288-6, Springer, 2019, https://doi.org/10.1007/978-3-030-24289-3_24

number of equations N is higher than the number of variables M. This linear system of equations can be solved by the least squares method (LSE) as

$$\boldsymbol{A}^T\boldsymbol{A}\boldsymbol{\lambda} = \boldsymbol{A}^T\boldsymbol{h}, \tag{6}$$

where the matrix $\boldsymbol{A}^T\boldsymbol{A}$ is symmetrical. Another possibility to solve the overdetermined system of linear equations $\boldsymbol{A}\boldsymbol{\lambda} = \boldsymbol{h}$ is using the QR decomposition.

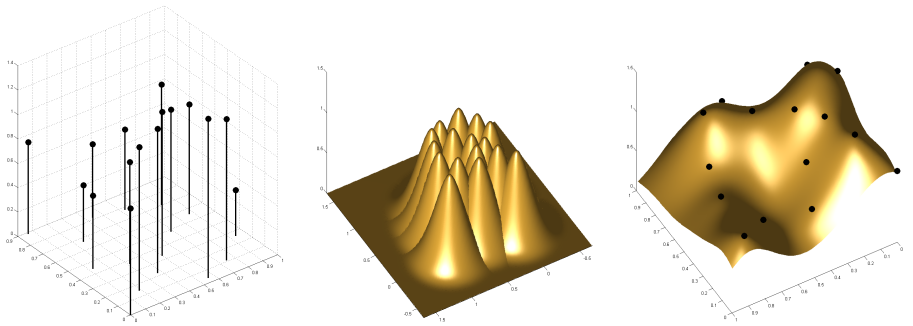

Fig. 1. Data values, the RBF collocation functions, the resulting interpolant (from [26]).

The RBF approximation can be done using "global" or "local" functions. When using "global" radial basis functions, the matrix $\boldsymbol{A}$ will be full and ill conditioned in general. When using "local" radial basis functions, the matrix $\boldsymbol{A}$ might be sparse, which can be beneficial when solving the overdetermined system of linear equations $\boldsymbol{A}\boldsymbol{\lambda} = \boldsymbol{h}$.

3 Proposed Approach

We propose a new approach for scattered data approximation of $2\frac{1}{2}D$ functions using Radial basis functions with respecting inflection points of the function. Inflection points are computed from the discrete mesh and from curves given by implicit points. For a simplicity, the proposed approach is demonstrated on sampled regular grid.

The input $2\frac{1}{2}D$ function $f(x, y)$ is for the sake of simplicity of evaluation sampled on a regular grid. For a general case neighbours have to be determined, e.g. by using a kd-tree. One important feature when computing the RBF approximation is the location of radial basis functions. We will show two main groups of locations, where the radial basis functions should be placed.

The first group are extreme points of the input data set. Most of the radial basis functions have the property of having its maximum at its center (we will

Computational Science and Its Application, ICSSA 2019 proceedings, Part I, LNCS 11619, pp.322-226, ISSN 0302-9743, ISBN 978-3-030-24288-6, Springer, 2019, https://doi.org/10.1007/978-3-030-24289-3_24

use only those) and thus it is very suitable to place the radial basis functions at the locations of extreme points.

The second group are inflection points of the input data set. The inflection points are important as the surface crosses its tangent plane, i.e. the surface changes from being concave to being convex, or vice versa. The surface at those locations should be approximated as accurately as possible in order to maintain the main features of the surface.

3.1 Determination of Extreme Points

The local extreme points of the function $f(x, y)$ can be either minimum or maximum, i.e.

$$\frac{\partial f}{\partial x} = 0 \quad \& \quad \frac{\partial f}{\partial y} = 0. \tag{7}$$

The decision if a point is a local extreme point can be done using only surrounding points. In our case, i.e. regular grid, we use four surrounding points, i.e. point on the right, left, up and down. In general case, neighbor points need to be determined, e.g. using a kd-tree. If a point is a local maximum, then all four surrounding points must be lower. The same also applies to a local minimum, i.e all four surrounding points must be higher.

4	6	8	6	5	4	3	4	5
5	7	6	5	5	2	1	3	5
6	8	7	7	4	3	2	2	4
9	4	4	5	5	4	4	3	5

Fig. 2. Location of local extreme points. The values 1 and 8 (green) are local extremes, i.e. local minimum and local maximum. The value 4 (red) is not a local extreme as the four surrounding values are higher and smaller as well.

The situation on the border of the input data set is a little bit different as we cannot use all four surrounding points, there will always be at least one missing. One solution is to skip the border of the input data set, however in this way we could omit some important extremes. Therefore, we determine the extremes from only three or two surrounding points.

3.2 Determination of Inflection Points

The second group of important locations for radial basis functions placement are inflection points, which forms actually curves of implicit points. The inflection

Computational Science and Its Application, ICSSA 2019 proceedings, Part I, LNCS 11619, pp.322-226, ISSN 0302-9743, ISBN 978-3-030-24288-6, Springer, 2019, https://doi.org/10.1007/978-3-030-24289-3_24

points are located where the Gaussian curvature is equal zero. The Gaussian curvature for $2\frac{1}{2}D$ function $f(x,y)$ is computed as

$$k_{gauss} = \frac{\frac{\partial^2 f}{\partial x^2}\frac{\partial^2 f}{\partial y^2} - \left(\frac{\partial^2 f}{\partial x \partial y}\right)^2}{\left(\left(\frac{\partial f}{\partial x}\right)^2 + \left(\frac{\partial f}{\partial y}\right)^2 + 1\right)^2}. \tag{8}$$

The Gaussian curvature is equal zero when

$$\frac{\partial^2 f}{\partial x^2}\frac{\partial^2 f}{\partial y^2} - \left(\frac{\partial^2 f}{\partial x \partial y}\right)^2 = 0. \tag{9}$$

This formula is equivalent to the calculation using the Hessian matrix, i.e.

$$\begin{vmatrix} \frac{\partial^2 f}{\partial x^2} & \frac{\partial^2 f}{\partial x \partial y} \\ \frac{\partial^2 f}{\partial y \partial x} & \frac{\partial^2 f}{\partial y^2} \end{vmatrix} = 0. \tag{10}$$

To find out the locations, where the Gaussian curvature, i.e. the determinant of Hessian matrix, is equal zero, we can sample the following function from the input discrete data set.

$$I(x,y) = \frac{\partial^2 f}{\partial x^2}\frac{\partial^2 f}{\partial y^2} - \left(\frac{\partial^2 f}{\partial x \partial y}\right)^2. \tag{11}$$

An application example of (11) can be seen in Fig. 3.

Now, we need to find out the locations, where this sampled function is equal zero. We again use the four surrounding points. If at least one is positive and at least one is negative, then there must be a zero value in between them. For the simplicity and to speed-up the calculation we consider the center point as the inflection point (see Fig. 3 and Fig. 4 for illustration).

4	6	8	6	5	4	-2	-3	-4
5	2	6	5	5	2	1	-1	-5
2	1	3	7	4	3	2	2	4
-2	-1	0	5	5	4	4	3	5

Fig. 3. Location of inflection points. The green positions with values 1 are considered as inflection points. The red position with value 4 is not an inflection point as all four surrounding values from (11) are positive.

The resulting inflection points form a curve of implicit points. It is quite densely sampled. However, for the purpose of the RBF approximation, we can

Computational Science and Its Application, ICSSA 2019 proceedings, Part I, LNCS 11619, pp.322-226, ISSN 0302-9743, ISBN 978-3-030-24288-6, Springer, 2019, https://doi.org/10.1007/978-3-030-24289-3_24

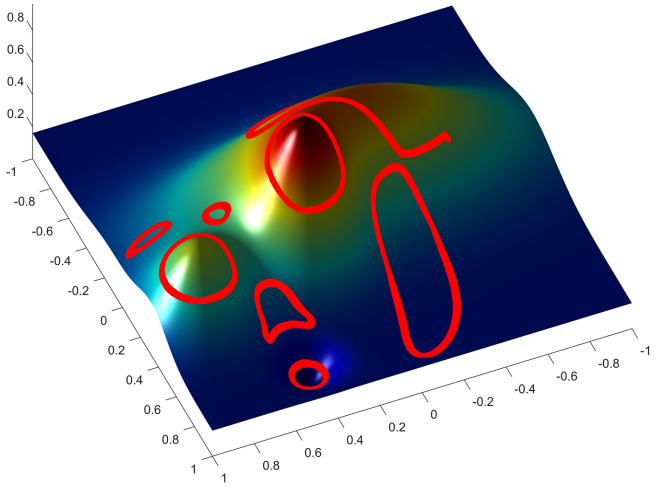

Fig. 4. An example of $2\frac{1}{2}D$ function with the curves of inflection points. The red curve represents the location of inflection points calculated using (11).

reduce the inflection points to obtain a specific number of inflection points or reduce them as the distance between the closest two is larger than some threshold value.

3.3 RBF Approximation with Respecting Inflection Points

In the previous chapters, we presented the location of radial basis functions for $2\frac{1}{2}D$ function approximation. These locations are well placed to capture the main shape of the function $f(x, y)$. However we should add some more additional points to cover the whole approximation space. One set of additional radial basis functions is placed on the border and in the corners. The last additional radial basis functions are placed at locations with Halton distribution [4]

$$Halton(p)_k = \sum_{i=0}^{\lfloor \log_p k \rfloor} \frac{1}{p^{i+1}} \left(\left\lfloor \frac{k}{p^i} \right\rfloor \bmod p \right), \tag{12}$$

where p is the prime number and k is the index of the calculated element, see Fig. 5 for an example of denerated points distribution. It is recommended to use different primes for x and y coordinate.

Knowing all the positions of radial basis functions, we can compute the RBF approximation of the $2\frac{1}{2}D$ function. For the calculation we use the approach described in Section 2.1.

Computational Science and Its Application, ICSSA 2019 proceedings, Part I, LNCS 11619, pp.322-226, ISSN 0302-9743, ISBN 978-3-030-24288-6, Springer, 2019, https://doi.org/10.1007/978-3-030-24289-3_24

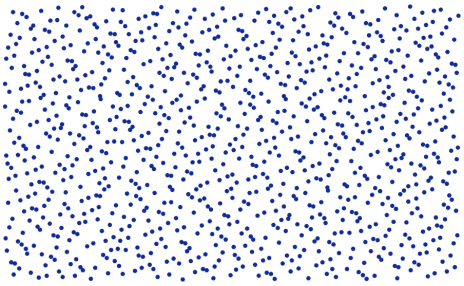

Fig. 5. The example of 10^3 Halton points. The Halton sequence was generated using two prime numbers $[2, 3]$, i.e. for x coordinates a Halton sequence with the prime number 2 and for y coordinates a Halton sequence with the prime number 3.

4 Experimental Results

In this section, we test the proposed approach for Radial basis function approximation. We tested the approach on all standard testing functions from [6]. In this paper we present the experimental results on only three testing functions, while the results for other testing functions are similar. The selected testing functions are the following

$$f_1(x,y) = \frac{2}{11}\left(\sin\left(4x^2+4y^2\right) - (x+y) + \frac{5}{2}\right) \tag{13}$$

$$\begin{aligned} f_2(x,y) = &\frac{3}{4}e^{-\frac{1}{4}((9x-2)^2+(9y-2)^2)} + \frac{3}{4}e^{-\frac{1}{49}(9x+1)^2-\frac{1}{10}(9y+1)^2} \\ &+ \frac{1}{2}e^{-\frac{1}{4}(9x-7)^2-\frac{1}{4}(9y-3)^2} - \frac{1}{5}e^{-(9x-4)^2-(9y-7)^2} \end{aligned} \tag{14}$$

$$f_3(x,y) = \frac{1}{9}\tanh\left(9y-9x\right)+1 \tag{15}$$

All testing functions $z = f(x,y)$ were "normalized" to the interval $x, y \in \langle -1, 1\rangle$ and the "height" z to $\langle 0, 1\rangle$ in order to easily compare the proposed approximation properties and approximation error for all testing functions and we used Gaussian radial basis function in all experiments.

$$\varphi(r) = e^{-\epsilon r^2}. \tag{16}$$

Only some representative results are presented in this chapter. The visualization of (13) is in Fig. 6, the visualization of (14) is in Fig. 9 and the visualization of (15) is in Fig. 12.

The first function (13) is an inclined sine wave. This function contains inflection points formed in the elliptical shapes as can be seen in Fig. 8b. In the experiments we used the Gaussian radial basis function with a shape parameter

Computational Science and Its Application, ICSSA 2019 proceedings, Part I, LNCS 11619, pp.322-226, ISSN 0302-9743, ISBN 978-3-030-24288-6, Springer, 2019, https://doi.org/10.1007/978-3-030-24289-3_24

$\epsilon = 1$. The visualization of original function together with the RBF approximation is in Fig. 6. The approximation consists of 246 radial basis functions (78 are at locations of inflection points and extremes, 24 are at the borders and 144 are Halton points). It can be seen that the RBF approximation is visualy identical to the original one. Also precision of approximation is very high, see Fig. 8a

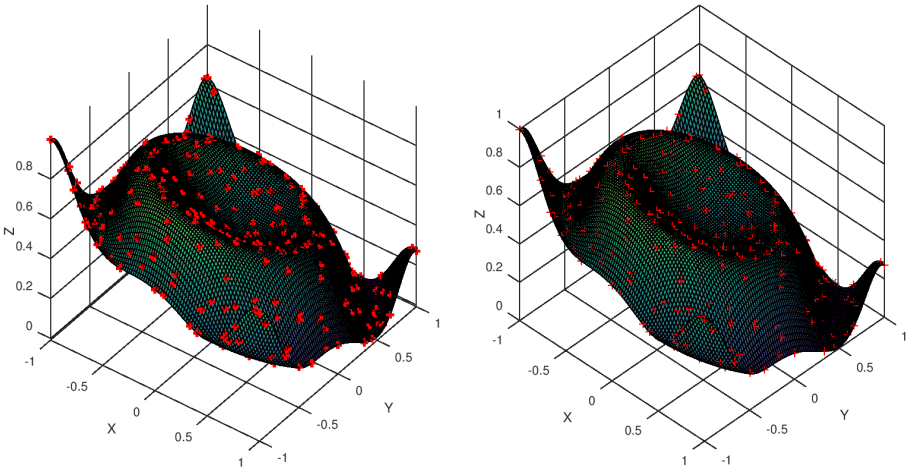

(a) Original data set. (b) RBF approximation.

Fig. 6. The RBF approximation of $2\frac{1}{2}D$ function (13). The total number of RBF centers is 246 (red marks).

To have a more closer look at the quality of RBF approximation, we computed the isocontours of the both original and approximated functions, see Fig. 7. Those isocontours are again visualy identical and cannot be seen any difference.

To compare the original and RBF approximated functions, we can compute the approximation error using the following formula for each point of evaluation.

$$Err = |f(x, y) - f_{RBF}(x, y)|, \tag{17}$$

where $f(x, y)$ is the value from input data set and $f_{RBF}(x, y)$ is the approximated value. Absolute error is used for evaluationas data are normalized to $\langle -1, 1\rangle \times \langle -1, 1\rangle \times \langle 0, 1\rangle$ as described recently. If we compute the approximation error for all input sample points, then we can calculate the average approximation error, which is $2.37 \cdot 10^{-4}$, and also the histogram of approximation error, see Fig. 8a. It can be seen that the most common approximation errors are quite low values below 0.4%. The higher approximation errors appear only few times. This proves a good properties of the approximation method.

The next testing function (14) is visualized together with the RBF approximation in Fig. 9. This function consists of four hills and the RBF approximation

Computational Science and Its Application, ICSSA 2019 proceedings, Part I, LNCS 11619, pp.322-226, ISSN 0302-9743, ISBN 978-3-030-24288-6, Springer, 2019, https://doi.org/10.1007/978-3-030-24289-3_24

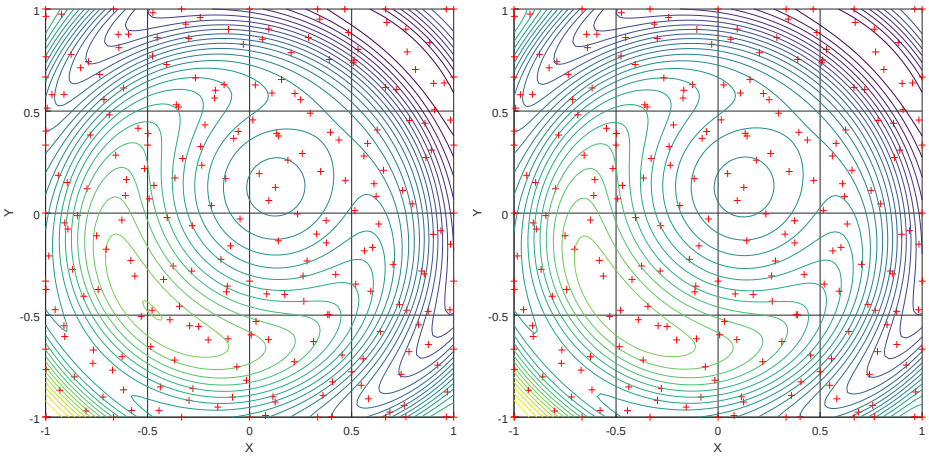

(a) Original data set. (b) RBF approximation.

Fig. 7. The comparison of function isocontours.

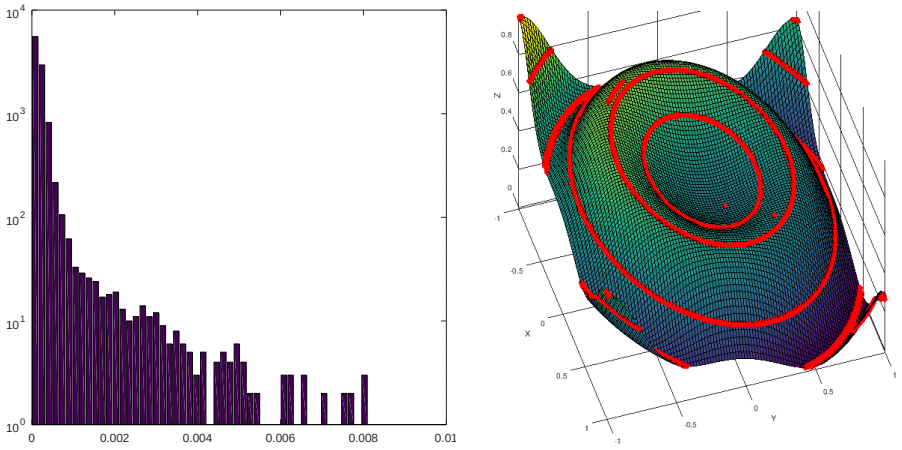

(a) Histogram of approximation error. (b) Inflection and extreme points.

Fig. 8. The histogram (a) of approximation error for the function (13). The horizontal axis represents the absolute approximation error computed as (17). It should be noted, that the vertical axis is in logarithmic scale. The visualization (b) of all located inflection and extreme points.

preserves the main shape. The only small difference is at the borders, which can be seen in more details in Fig. 10. The Gauss function with the shape parameter $\epsilon = 26$ was used as radial basis function.

Computational Science and Its Application, ICSSA 2019 proceedings, Part I, LNCS 11619, pp.322-226, ISSN 0302-9743, ISBN 978-3-030-24288-6, Springer, 2019, https://doi.org/10.1007/978-3-030-24289-3_24

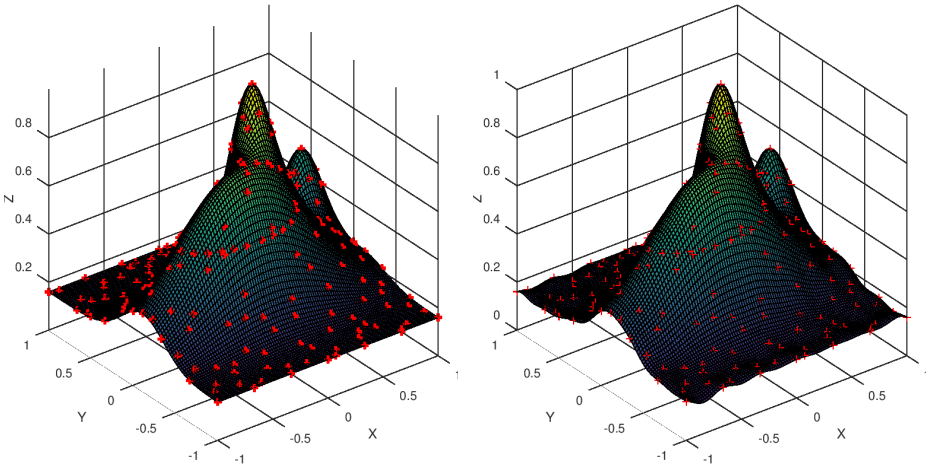

(a) Original data set. (b) RBF approximation.

Fig. 9. The RBF approximation of $2\frac{1}{2}D$ function (14). The total number of RBF centers is 244 (red marks).

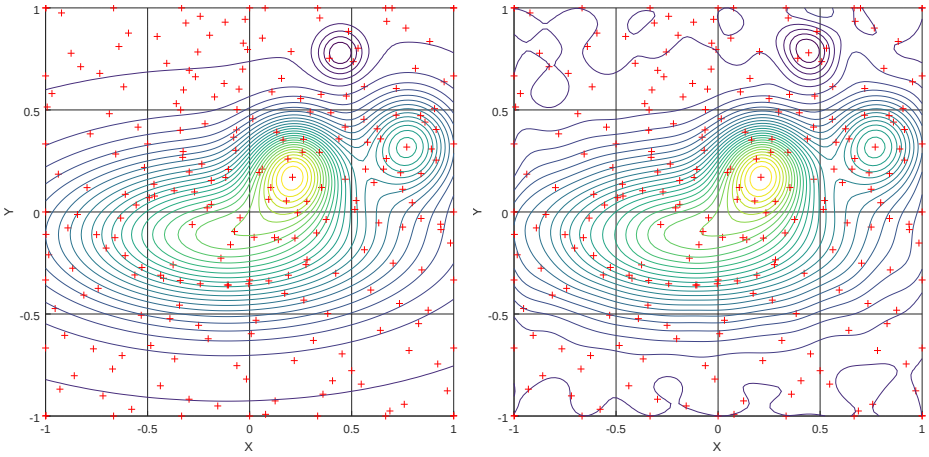

(a) Original data set. (b) RBF approximation.

Fig. 10. The comparison of function isocontours.

The average approximation error is $2.75 \cdot 10^{-3}$ and the distribution of the approximation error can be seen in the histogram in Fig. 11.

The last function (15) for testing the proposed RBF approximation is visualized in Fig. 12a. This function is quite exceptional, because it has a sharp cliff on $x = y$. Such sharp cliffs are always very hard to approximate using the RBF.

Computational Science and Its Application, ICSSA 2019 proceedings, Part I, LNCS 11619, pp.322-226, ISSN 0302-9743, ISBN 978-3-030-24288-6, Springer, 2019, https://doi.org/10.1007/978-3-030-24289-3_24

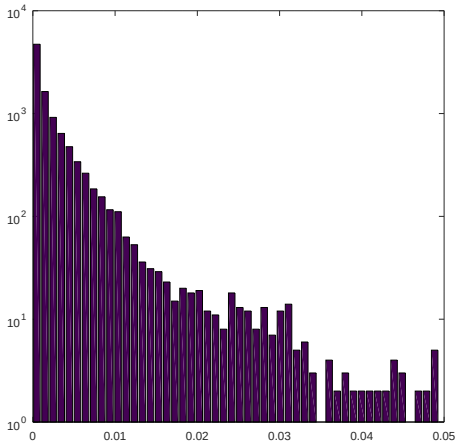

Fig. 11. The histogram of approximation error for the function (14). The horizontal axis represents the absolute approximation error computed as (17). It should be noted, that the vertical axis is in logarithmic scale.

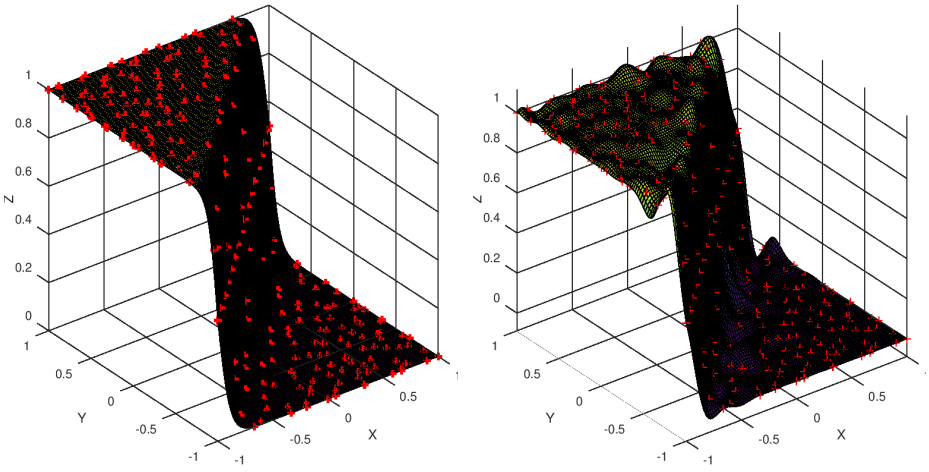

(a) Original data set. (b) RBF approximation.

Fig. 12. The RBF approximation of $2\frac{1}{2}D$ function (15). The total number of RBF centers is 244 (red marks).

However using the proposed distribution of the radial basis functions, we are able to approximate the sharp cliff quite well, see Fig. 12b. The problem, that comes up, is the wavy surface for $y > x$, see more details in Fig. 13. The Gauss function with the shape parameter $\epsilon = 25$ was used as the radial basis function.

Computational Science and Its Application, ICSSA 2019 proceedings, Part I, LNCS 11619, pp.322-226, ISSN 0302-9743, ISBN 978-3-030-24288-6, Springer, 2019, https://doi.org/10.1007/978-3-030-24289-3_24

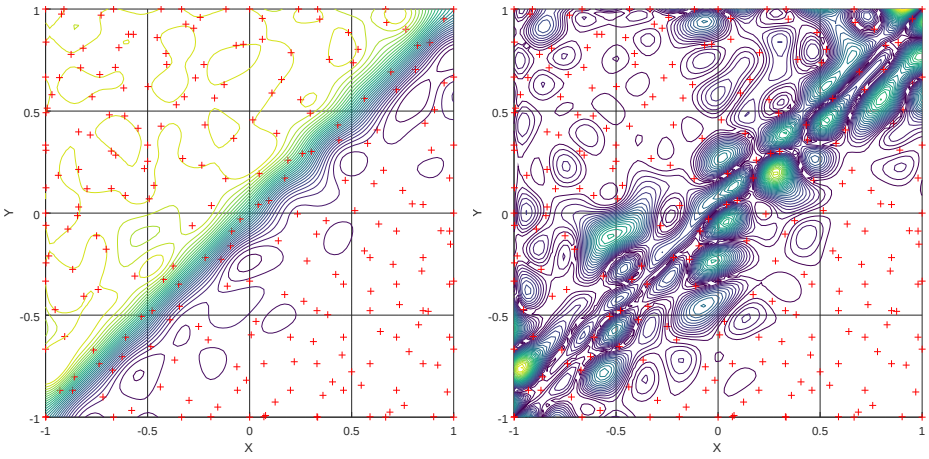

(a) RBF approximation isocontours. (b) Approximation error isocontours.

Fig. 13. The visualization of approximated function isocontours (a). The visualization of approximation error as isocontours plot (b), please note that the average approximation error is $1.22 \cdot 10^{-2}$.

The average approximation error for this specific function is $1.22 \cdot 10^{-2}$. This result is quite positive as the function is very hard to approximate using the RBF approximation technique. The histogram of the approximation error is visualized in Fig. 14.

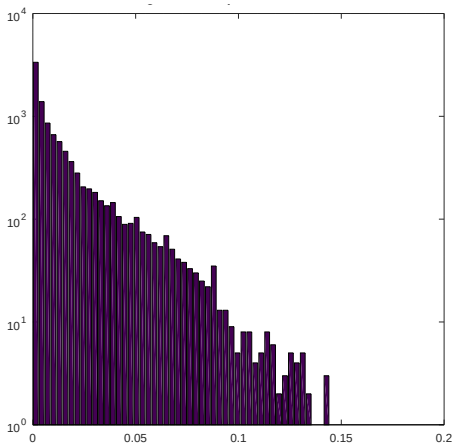

Fig. 14. The histogram of approximation error for the function (15). The horizontal axis represents the absolute approximation error computed as (17). It should be noted, that the vertical axis is in logarithmic scale.

Computational Science and Its Application, ICSSA 2019 proceedings, Part I, LNCS 11619, pp.322-226, ISSN 0302-9743, ISBN 978-3-030-24288-6, Springer, 2019, https://doi.org/10.1007/978-3-030-24289-3_24

5 Conclusion

We presented a new approach for approximation of $2\frac{1}{2}D$ scattered data using Radial basis functions respecting inflection points in the given data set. The RBF approximation uses the properties of the input data set, namely the extreme and the inflection points to determine the location of radial basis functions. This sophisticated placement of radial basis functions significantly improves the quality of the RBF approximation. It reduces the needed number of radial basis functions and thus creates even more compressed RBF approximation, too.

In future, the proposed approach is to be extended to approximate $3\frac{1}{2}D$ scattered data, while utilizing the properties of the input data set for the optimal placement of radial basis functions. Also efficient finding a shape parameters is to be explored.

Acknowledgments

The authors would like to thank their colleagues at the University of West Bohemia, Plzen, for their discussions and suggestions, and anonymous reviewers for their valuable comments and hints provided. The research was supported by projects Czech Science Foundation (GACR) No. 17-05534S and partially by SGS 2019-016.

References

1. F. Afiatdoust and M. Esmaeilbeigi. Optimal variable shape parameters using genetic algorithm for radial basis function approximation. *Ain Shams Engineering Journal*, 6(2):639–647, 2015.
2. J. Biazar and M. Hosami. Selection of an interval for variable shape parameter in approximation by radial basis functions. *Advances in Numerical Analysis*, 2016, 2016.
3. S. Chen, E. Chng, and K. Alkadhimi. Regularized orthogonal least squares algorithm for constructing radial basis function networks. *International Journal of Control*, 64(5):829–837, 1996.
4. G. E. Fasshauer. *Meshfree approximation methods with MATLAB*, volume 6. World Scientific, 2007.
5. B. Fornberg and G. Wright. Stable computation of multiquadric interpolants for all values of the shape parameter. *Computers & Mathematics with Applications*, 48(5-6):853–867, 2004.
6. R. Franke. A critical comparison of some methods for interpolation of scattered data. Technical report, Naval Postgraduate School Monterey CA, 1979.
7. S. Ghosh-Dastidar, H. Adeli, and N. Dadmehr. Principal component analysis-enhanced cosine radial basis function neural network for robust epilepsy and seizure detection. *IEEE Transactions on Biomedical Engineering*, 55(2):512–518, 2008.
8. R. L. Hardy. Multiquadric equations of topography and other irregular surfaces. *Journal of geophysical research*, 76(8):1905–1915, 1971.

Computational Science and Its Application, ICSSA 2019 proceedings, Part I, LNCS 11619, pp.322-226, ISSN 0302-9743, ISBN 978-3-030-24288-6, Springer, 2019, https://doi.org/10.1007/978-3-030-24289-3_24

9. R. L. Hardy. Theory and applications of the multiquadric-biharmonic method 20 years of discovery 1968–1988. *Computers & Mathematics with Applications*, 19(8-9):163–208, 1990.
10. A. Karim and H. Adeli. Radial basis function neural network for work zone capacity and queue estimation. *Journal of Transportation Engineering*, 129(5):494–503, 2003.
11. E. Larsson and B. Fornberg. A numerical study of some radial basis function based solution methods for elliptic PDEs. *Computers & Mathematics with Applications*, 46(5):891–902, 2003.
12. Z. Majdisova and V. Skala. Big geo data surface approximation using radial basis functions: A comparative study. *Computers & Geosciences*, 109:51–58, 2017.
13. Z. Majdisova and V. Skala. Radial basis function approximations: Comparison and applications. *Applied Mathematical Modelling*, 51:728–743, 2017.
14. Z. Majdisova, V. Skala, and M. Smolik. Determination of stationary points and their bindings in dataset using rbf methods. In *Proceedings of the Computational Methods in Systems and Software*, pages 213–224. Springer, 2018.
15. M. J. Orr. Regularised centre recruitment in radial basis function networks. In *Centre for Cognitive Science, Edinburgh University*. Citeseer, 1993.
16. M. J. Orr. Regularization in the selection of radial basis function centers. *Neural computation*, 7(3):606–623, 1995.
17. R. Pan and V. Skala. A two-level approach to implicit surface modeling with compactly supported radial basis functions. *Engineering with Computers*, 27(3):299–307, 2011.
18. R. Pan and V. Skala. Surface reconstruction with higher-order smoothness. *The Visual Computer*, 28(2):155–162, 2012.
19. G. Prakash, M. Kulkarni, and U. Sripati. Using RBF neural networks and Kullback-Leibler distance to classify channel models in free space optics. In *Optical Engineering (ICOE), 2012 International Conference on*, pages 1–6. IEEE, 2012.
20. S. A. Sarra and D. Sturgill. A random variable shape parameter strategy for radial basis function approximation methods. *Engineering Analysis with Boundary Elements*, 33(11):1239–1245, 2009.
21. I. P. Schagen. Interpolation in two dimensions - a new technique. *IMA Journal of Applied Mathematics*, 23(1):53–59, 1979.
22. V. Skala. Fast interpolation and approximation of scattered multidimensional and dynamic data using radial basis functions. *WSEAS Transaction on Mathematics*, 12(5):501–511, 2013.
23. V. Skala. RBF interpolation with CSRBF of large data sets. *Procedia Computer Science*, 108:2433–2437, 2017.
24. M. Smolik and V. Skala. Spherical rbf vector field interpolation: experimental study. In *2017 IEEE 15th International Symposium on Applied Machine Intelligence and Informatics (SAMI)*, pages 000431–000434. IEEE, 2017.
25. M. Smolik and V. Skala. Large scattered data interpolation with radial basis functions and space subdivision. *Integrated Computer-Aided Engineering*, 25(1):49–26, 2018.
26. M. Smolik, V. Skala, and Z. Majdisova. Vector field radial basis function approximation. *Advances in Engineering Software*, 123(1):117–129, 2018.
27. M. Smolik, V. Skala, and O. Nedved. A comparative study of LOWESS and RBF approximations for visualization. In *International Conference on Computational Science and Its Applications*, pages 405–419. Springer, 2016.

Computational Science and Its Application, ICSSA 2019 proceedings, Part I, LNCS 11619, pp.322-226, ISSN 0302-9743, ISBN 978-3-030-24288-6, Springer, 2019, https://doi.org/10.1007/978-3-030-24289-3_24

28. K. Uhlir and V. Skala. Reconstruction of damaged images using radial basis functions. In *Signal Processing Conference, 2005 13th European*, pages 1–4. IEEE, 2005.
29. J. Wang and G. Liu. On the optimal shape parameters of radial basis functions used for 2-d meshless methods. *Computer methods in applied mechanics and engineering*, 191(23-24):2611–2630, 2002.
30. H. Wendland. Computational aspects of radial basis function approximation. *Studies in Computational Mathematics*, 12:231–256, 2006.
31. G. B. Wright. Radial basis function interpolation: Numerical and analytical developments. 2003.
32. L. Yingwei, N. Sundararajan, and P. Saratchandran. Performance evaluation of a sequential minimal radial basis function (RBF) neural network learning algorithm. *IEEE Transactions on neural networks*, 9(2):308–318, 1998.
33. X. Zhang, K. Z. Song, M. W. Lu, and X. Liu. Meshless methods based on collocation with radial basis functions. *Computational mechanics*, 26(4):333–343, 2000.